ARTICLE

Ammonia-assisted reforming and dehydrogenation toward efficient light alkane conversion

Received 00th January 20xx, Accepted 00th January 20xx

DOI: 10.1039/x0xx00000x

Yizhi Xiang*a

The proven world reserves of natural gas are up to 7400 trillion cubic feet, providing cheap and abundant light alkane as feedstocks for chemicals and energy syntheses. However, efficient conversion of light alkane (with inert C-H and C-C bonds) to value-added chemicals with more active functional groups remains a formidable challenge. The conventional catalytic reactions, including steam/dry reforming, oxidative/non-oxidative dehydrogenation, dehydroaromatization, and partial oxidation, have been extensively studied for light alkane conversion. Whereas, alternative catalytic systems, such as ammonia-assisted reforming and dehydrogenation have been less concerned. Green ammonia from renewable energy has been considered as an important energy carrier, therefore, it could be an important co-reactant for light alkane conversion. This perspective highlights the essentials of ammonia reforming (for CO_x-free H₂ and HCN) and dehydrogenation (for acetonitrile and H₂) as alternative catalytic processes for efficient light alkane conversion.

1. Introduction

The proven world reserves of natural gas are increasing continuously. According to the U.S. Energy Information Administration, the estimated total world proved reserves of natural gas is up to 7,257 trillion cubic feet (Tcf)as of January 1, 2020.¹ In the United States alone, the natural gas reservation increased from 473.3 Tcf at year-end of 2020 to 625.4 Tcf by the year-end of 2021 (an increase of 33%), establishing a new record for natural gas proved reserves.² The unprecedented increase in natural gas reservation and production provides cheap and abundant light alkane as alternative feedstocks to crude oil for chemicals and energy syntheses. Consequently, researchers from both academia and industry dedicated considerable efforts to the development of more efficient catalytic systems for light alkane selective conversions.

Significant achievements were made during the past decade regarding the catalyst design and process innovation for efficient light alkane conversion, mainly for conventional steam-/dry-reforming,³⁻⁸ oxidative/non-oxidative dehydrogenation,⁹⁻ ¹⁷ partial oxidation, ¹⁸⁻²⁵ and dehydroaromatization. ²⁶⁻³⁷ For example, the McFarland group reported the simultaneous pyrolysis and dry reforming of methane in a bubble column reactor using a molten Ni/In alloy catalyst.⁴ The H₂ to CO ratio can be adjusted by changing the CH₄ to CO₂ feed ratio considering that pyrolysis of methane produces H2 and solid carbon (separable from the molten metal). Yavuz group and highly cokingsintering-resistant developed а molybdenum-doped nickel catalyst for methane dry reforming,6 which was achieved by stabilizing the nanocatalyst on the edge

Besides the mentioned achievements in the conventional catalytic reaction processes, light alkane can also be converted into value-added chemicals through alternative catalytic reactions, such as ammonia (NH₃)-assisted catalytic reactions, including ammoxidation and ammonia reforming (AmmoReform). In industry, these catalytic processes were employed for nitrogen-containing compounds, such as acrylonitrile and hydrogen cyanide (HCN) production. For example, the ammoxidation of propylene is an industrial reaction for acrylonitrile production. In such a process, propylene, ammonia, and air are passed through a fluidized bed reactor containing the bismuth phosphomolybdate catalyst at 400-510 °C and 50-200 kPa. The process was initially invented in the 1950s by the Standard Oil of Ohio, therefore also known as the "SOHIO Process".38 The SOHIO process co-produces acetonitrile (ACN) and HCN as the by-products, which is the only

of a single-crystalline magnesium oxide support. Ryoo group developed rare-earth-platinum alloy nanoparticles (in zeolite),9 Sykes and co-workers developed a RhCu single atom alloy catalyst,¹⁰ Bell group developed an isolated Pt in ≡SiOZn-OH nests (in dealuminated beta zeolite) catalyst,12 Notestein and coworkers developed an In₂O₃-Pt/Al₂O₃ catalyst,¹³ and Xiao group developed isolated boron in zeolite catalyst, 15 for the efficient oxidative/non-oxidative propane dehydrogenation. For light alkane partial oxidation to oxygenated products, the Flytzani-Stephanopoulos group developed a single-atom Rh catalyst in zeolite for methane oxidation to methanol or acetic acid.18 van Bokhoven group studied the anaerobic oxidation of methane using CuMOR catalyst. 19 Xiao group developed a hydrophobic zeolite for methane oxidation to methanol by the H_2O_2 .²¹ in-situ formed Concerning light dehydroaromatization, a recent study in our group developed a binary PtZn@HZSM-5 catalyst (with Pt loading as low as 10 ppm), which shown outstanding activity and stability.³⁷

^a· Dave C. Swalm School of Chemical Engineering, Mississippi State University, Mississippi State, MS, 39762, USA. Email: <u>yzxianq@che.msstate.edu</u>

current industrial source of ACN. Another important catalytic reaction between light alkane and ammonia is related to HCN production through either the Degussa^{39, 40} or the Andrussow⁴⁰ process. The Degussa process – also known as the Bläusaure aus Methan und Ammoniak (BMA) process – is a highly endothermic nonoxidative reaction that was performed at temperatures ≥1200 °C in alumina tube bundles (coated with Pt).41-43 Whereas, the Andrussow process is an oxidative and exothermic reaction, and it is a more common process for HCN production in the industry.44-47 The Andrussow reaction is performed on the Pt-Rh gauze (20-50 layer) and the reactor operates adiabatically at ≥1100 °C. Besides the BMA and Andrussow processes, which mainly employ methane as the feedstock, the industry Shawinigan process employs propane as the feedstock for HCN production. 40, 48, 49 The Shawinigan HCN reactor consists of a refractory lined electrically heated vessel and operates at 1300-1600 °C in the absence of a catalyst. 48

While ammonia-assisted light alkane conversions are conventionally only employed for HCN and acrylonitrile production in industry, new opportunities are emerging for these traditional catalytic reactions due to the prospects for green ammonia as an energy carrier. Ammonia is a highdemand chemical commodity not only owing to its use in agriculture but also because it is a potential chemical vector for renewable energy storage and transportation.⁵⁰ Indeed, ammonia as a carbon-free H₂ carrier has been extensively recognized recently,51-53 and many green ammonia factories have been built or under building worldwide.54-57 As green ammonia becomes ubiquitously available from renewable energy, the ammonia-assisted catalytic conversions of light alkane might be employed as platform reactions for chemical and energy transformation. This perspective focuses on C₁-C₃ light alkane conversion and addresses the opportunities and challenges of ammonia-assisted reforming (for CO_x-free H₂ and HCN) and dehydrogenation (ammonia/ethane dehydrogenative C-N coupling for ACN and H₂) as alternative catalytic processes for efficient light alkane conversion.

2. Ammonia reforming for CO_x-free H₂ or HCN

2.1 Ammonia reforming as analogous to steaming reforming

The concept of ammonia reforming (AmmoReform) for light alkane upgrading – for CO_x -free H_2 production – was recently proposed in our group. Such a catalytic process is closely related to the BMA and Shawinigan processes from the reaction stoichiometric. Taking ethane AmmoReform as an example, the stoichiometric reaction is shown in equation (1).

$$C_2H_6 + 2NH_3 \rightarrow 2HCN + 5H_2 \quad \Delta H^{\circ} = 89.4 \text{ kJ/mol}_{H_2}$$
 (1)

Such a reaction is similar to conventional steam reforming (SteamReform, see equation (2)) if ammonia is written as " H_2NH ", where "NH" is analogous to "O" in water molecular.

$$C_2H_6 + 2H_2O(g) \rightarrow 2CO + 5H_2 \Delta H^{\circ} = 69.4 \text{ kJ/mol}_{H_2}$$
 (2)

Although the AmmoReform shows a higher standard state reaction enthalpy change ΔH^{e} (at 25^{o}C) than the SteamReform, considering the latent heat for steam generation (40.9 kJ/mol

at 1 atm and 100 °C), the two processes show quite similar reaction endothermicity. Noteworthily, with increasing temperature, the ΔH^e of AmmoReform increases, whereas the ΔH^e of SteamReform decreases. Therefore, under the reaction conditions, the AmmoReform is more endothermicity.

Additionally, the AmmoReform of ethane also shares the same types of side reactions as the ethane SteamReform, which include ethane hydrogenolysis/cracking (equations (3) and (4)), and HCN or CO hydrogenation (equations (5) and (6)). These side reactions all produce CH₄ as the by-product. Nonetheless, the reaction system becomes simple for methane AmmoReform (reversible equation (5)) and SteamReform (reversible equation (6)) due to the absence of equations (3) and (4).

$$C_2H_6 + H_2 \rightarrow 2CH_4$$
 $\Delta H^{\circ} = -64.5 \text{ kJ}$ (3)

$$C_2H_6 \rightarrow CH_4 + C + H_2$$
 $\Delta H^{\circ} = 10 \text{ kJ}$ (4)

$$HCN + 3H_2 \rightarrow CH_4 + NH_3$$
 $\Delta H^{\circ} = -256 \text{ kJ}$ (5)

$$CO + 3H_2 \rightarrow CH_4 + H_2O(1)$$
 $\Delta H^{\circ} = -250 \text{ kJ}$ (6)

Unlike SteamReform, ammonia decomposition (equation (7)) is a unique side reaction of the AmmoReform process. The ammonia decomposition produces additional H_2 , therefore, it is an advantage if CO_x -free H_2 is the target product, however, is not desired if such a reaction aims at HCN production due to the decreased HCN selectivity (nitrogen-based).

$$2NH_3 \rightarrow N_2 + 3H_2 \qquad \Delta H^{\circ} = 92 \text{ kJ} \tag{7}$$

The thermodynamic (Gibbs free reaction energy (ΔG) \sim temperature under atmospheric pressure) of the involved reactions is shown in Fig. 1. It is seen that the AmmoReform is thermodynamically less favorable than the SteamReform.

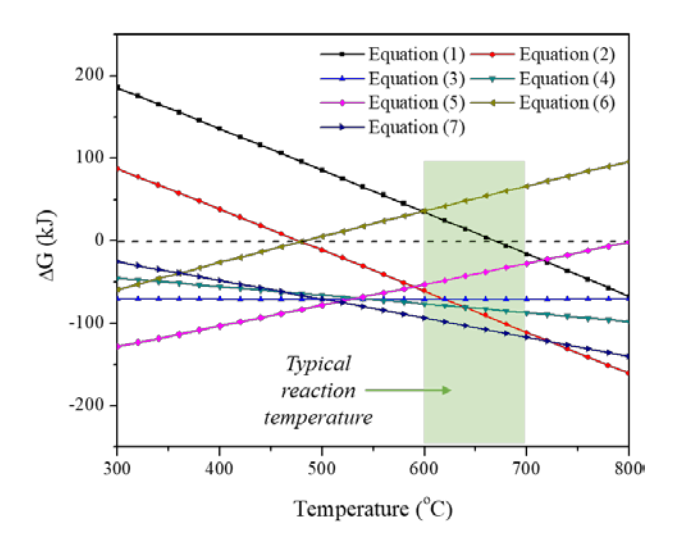


Figure 1 Gibbs free energy change as a function of reaction temperature for equations (1)-(7). Calculated using HSC Chemistry 6.0

The free energy ΔG decreases with increasing temperature for both AmmoReform and SteamReform and the temperatures at which $\Delta G = 0$ for ethane AmmoReform and SteamReform are ~477.6 °C and ~668 °C, respectively. In order to obtain a higher ethane conversion, a reaction temperature above 600 °C is required. All of the side reactions (equations (3)-(5) and (7))

have negative ΔG at temperatures between 300-800 ${}^{\Omega}C$, indicating that the formation of unwanted CH₄ and ammonia decomposition are thermodynamically preferred. Nonetheless, these reactions are typically limited by reaction kinetic rather than thermodynamic. Therefore, the development of highly active and selective catalysts is ultimately important to both the AmmoReform and SteamReform of ethane.

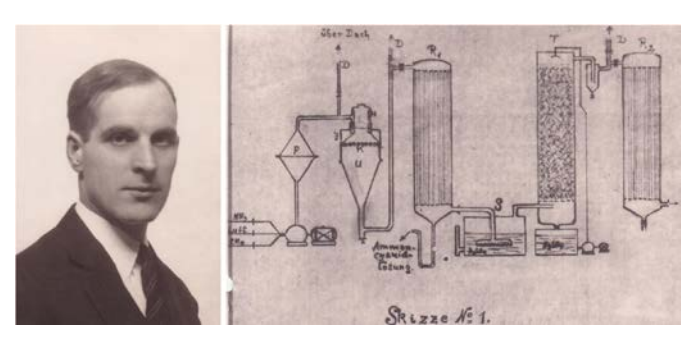


Figure 2 Dr. Leonid Andrussow (1896-1986) and process description for his hydrocyanic acid synthesis from methane and ammonia (1930). Reproduced with permission from Wikipedia (https://en.wikipedia.org/wiki/Leonid Andrussow and https://en.wikipedia.org/wiki/Andrussow process), Hermann Luyken/CC-BY-SA 3.0, https://creativecommons.org/licenses/by-sa/3.0/deed.en.

2.2 Conventional ammonia reforming: the BMA process

The Degussa BMA process is one of the conventional methane AmmoReform (the reverse reaction of equation (5)) processes that aim at HCN production. The reaction is highly endothermic and requires a high reaction temperature ≥1200 °C. The reaction is performed in alumina tube bundles that are coated with a thin layer of a special Pt catalyst.⁴¹⁻⁴³ Due to the high

endothermicity of the reaction at such a high temperature, the alumina tube reactors are externally heated by a large gasburner furnace,^{59, 60} which is the same as the methane SteamReform process for syngas production. 61 The specific energy consumption of the BMA process is up to 4×10⁴ kJ/kg HCN,⁴⁹ therefore, it is highly energy intensive. To avoid coke deposition on the tube, an off-stoichiometric NH₃/CH₄ ratio (~1.07) is used to maintain a slightly carbon-lean condition. After leaving the reaction tubes, the product gas is cooled to 300 °C by passing through a water-cooled heater exchange. After that, the gas is washed with dilute sulfuric acid to remove unreacted ammonia, which is essential to prevent the polymerization of HCN. After the ammonia scrubber, the gas then is passed through an adsorption column, where HCN is adsorbed by cold water. The overall process is similar to the Andrussow process pioneered by Leonid Andrussow (Fig. 2) at BASF's ammonia laboratory. Noteworthily, the Andrussow process, which can be considered as ammoxidation or oxidative AmmoReform of methane (CH₄ + NH₃ + 1.5O₂ \rightarrow HCN + 3H₂O), will not be discussed in detail in the perspective. During the industrial BMA process, about 80-87% of the NH₃ and 90-94% of CH₄ are converted into HCN. Although the tail gas consists mainly of pure H₂, it is frequently burned for heating the furnace during the conventional BMA process. Additionally, the C3+ alkanes, such as propane and iso-/n-butane, were studied for the BMA process, but a stoichiometric amount of H2 co-feed is required for hydrogenolysis (to CH₄).⁵⁹ It seems that with C₂₊ alkanes as the reactant for the BMA process, the catalyst fouling is, even more, significant.59

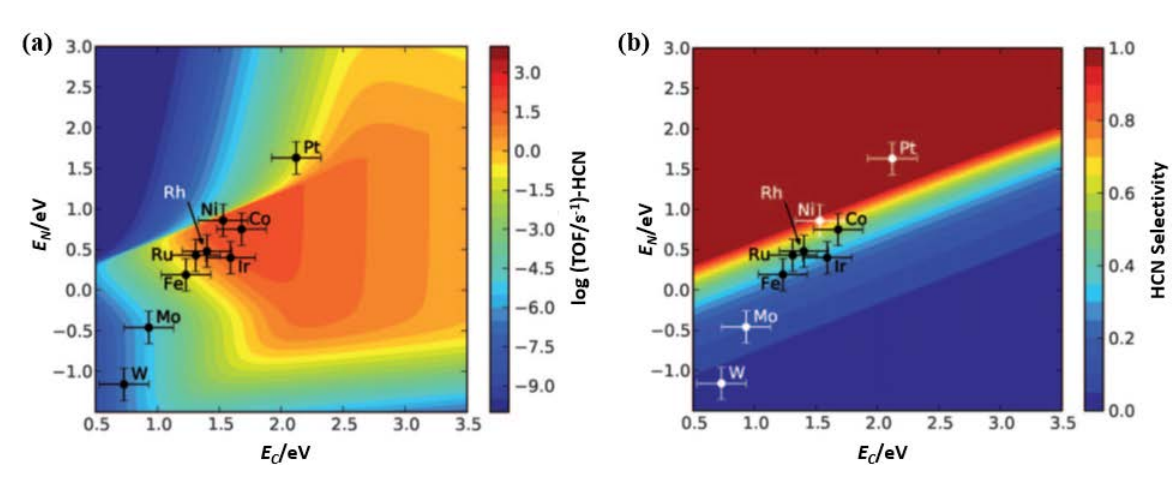


Figure 3 Calculated logarithmic turnover frequency (TOF) for (a) HCN production and (b) selectivity towards HCN production as a function of the carbon (E_c) and nitrogen (E_N) binding energies. Reproduced from ref. 63 with permission from John Wiley and Sons, Copyright © 2011 WILEY-VCH Verlag GmbH & Co. KGaA, Weinheim.

2.3 The conventional catalyst and mechanism

The Pt metal is the key catalytically active component for the conventional BMA process. The catalyst consisting essentially of aluminum oxide contains platinum and aluminum nitride is coated on the alumina tube with a Pt density of 10-30 mg/cm 2 . Find the coated catalyst after drying is reduced with hydrogen at 600-900 $^{\circ}$ C and the nitride is formed during the induction period of the AmmoReform reaction through nitridation.

Without Pt, the Al_2O_3 or AlN itself is also active for AmmoReform at the temperatures for the BMA process. ⁶² However, in the absence of Pt, ammonia is mainly decomposed to N_2 and H_2 if methane is not in large excess, and a great surplus of methane would lead to significant coke formation. Therefore, the Al_2O_3 catalyst shows neither satisfactory yields nor acceptable lifetimes for the AmmoReform. Besides Pt, various other platinum group metals, such as Rh, Ru, Pd, Os, and Ir, as well as the nonnoble metal, including Ni and Cu, which alone or

in the form of alloy with each other are also suggested to be active for the AmmoReform at the BMA temperature. However, detailed activity data of these catalysts were absent from their early patent.60 More recently, Nørskov and coworkers calculated the influence of carbon and nitrogen binding energy on the catalytic behavior of methane AmmoReform over the various transition metal (211) surfaces.⁶³ As shown in Fig. 3, while Co, Ni, and Ir are found to be close to the top of the volcano (Fig. 3(a)), the commercial BMA catalyst, namely the Pt, is unique in terms of its high selectivity (Fig. 3(b)) towards HCN production. Additionally, Rh and Ru are also predicted to be more active than Pt in terms of HCN production, however, they show lower HCN selectivity. Pt is the only metal of those considered that produces only HCN, all of the other metals produce significant amounts of N2 through ammonia decomposition. Finally, Mo and W are predicted to be inactive and nonselective towards HCN production through methane AmmoReform.

While studies on the catalyst development for the AmmoReform are rather limited, the mechanism of HCN synthesis over the Pt-based catalyst has been subjected to numerous studies. Koberstein studied methane AmmoReform in a bench-scale Degussa BMA reactor using a Pt catalyst. 42 The flow type, heat, and mass transfer, as well as a macrokinetic model, were estimated.⁴² Schmidt and coworkers studied the kinetics of HCN synthesis from methane AmmoReform under UHV (0.05-5.0 Torr) conditions at temperatures between 500 and 1500 K on a polycrystalline Pt and Rh foil. 64, 65 According to their studies, the reactive Rh and Pt surfaces are covered with almost one monolayer of carbon, which reacts with NH_y fragments to give HCN. However, the catalyst would deactivate if multiple carbon layers were formed, indicating that the C-N coupling could occur between CH_x and NH_y species. Therefore, the rates of HCN formation are fit accurately by a modified Langmuir-Hinshelwood model that assumes surface carbon as both a reactant and a catalyst poison.

$$r_{HCN} = \frac{k_{HCN} P_{CH_4} P_{NH_3}^{0.5}}{\left(1 + K P_{CH_4} / P_{NH_3}^{0.5}\right)^{n+1}}$$

The rate constant k_{HCN} and equilibrium constant K were found by fitting the data to the model.

$$k_{HCN} = 7.8 \times 10^{18} e^{-1950/T}$$
 $K = 0.044 e^{2390/T}$

Herceg and Trenary suggested the direct coupling of C and N atoms on Pt (111) for the surface CN formation. 66 , 67 The conclusion was addressed based on the reflection absorption infrared spectroscopy (RAIRS) and temperature-programmed desorption (TPD) under UHV with CH $_{\rm 3}$ I and NH $_{\rm 3}$ as the precursors. Their results show that HCN desorption at $\sim\!500$ K is kinetically limited by the formation of the C-N bond at this temperature and high coverages of C $_{\rm ads}$ suppress CN formation. Delagrange and Schuurman performed temporal analysis of products (TAPs) experiments on Pt black for methane AmmoReform at 1173 K. 43 Their results show that ammonia decomposition is the rate-limiting step and HCN is formed by a C-N or HC-N coupling reaction. Consequently, the selectivity is

governed by CH₄ adsorption: fast CH₄ adsorption favors the formation of HCN while N₂ formation is hindered. Schwarz and coworkers studied the mechanisms of the gas phase Pt⁺mediated C-N coupling. The reaction was initiated by Pt⁺ dehydrogenates CH₄ to yield PtCH₂⁺, which reacts with gas phase NH₃ and yields various intermediates. The major pathway resulted in the formation of PtH and CH₂NH₂⁺ (PtCH₂⁺ + NH₃ \rightarrow PtH + CH₂NH₂⁺) and such a reaction is found to be exothermic by 23 kcal/mol. Noteworthily, dehydrogenation of NH₃ by Pt⁺ is endothermic and does not occur experimentally. Additionally, Pt⁺ is unique with respect to its ability to activate CH₄ and mediate C-N bond coupling in contrast to the transition metal cations (Fe⁺, Co⁺, Rh⁺, W⁺, Os⁺, Ir⁺, and Au⁺). Pt⁺

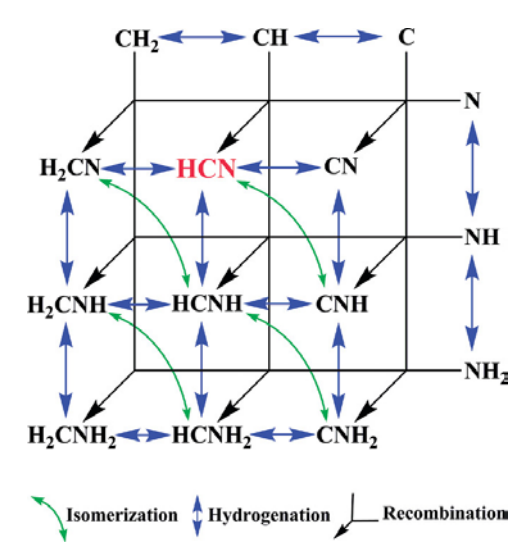


Figure 4 Reaction network leading to HCN on Pt (111) from methane AmmoReform. Reproduced from ref. 70 with permission from American Chemical Society, Copyright © 2011 American Chemical Society.

Besides the aforementioned experimental studies, Gómez-Díaz and López performed DFT calculations for the full reaction path leading to HCN formation from CH₄ and NH₃ on Pt (111). A complete reaction network leading to HCN formation, which includes dehydrogenation, H_x C-NH $_y$ (x = 0-2, y = 0-2) couplings, de/hydrogenation of C-N-containing species, and isomerization, is shown in Fig. 4. It was concluded that the C-N formation takes place through partially hydrogenated compounds, in particular, those coming from H_x C + NH $_2$ (x = 0, 1) coupling with subsequent dehydrogenation of the resulting intermediate; and the dehydrogenation of the HCNH $_2$ intermediate is the rate-limiting step in the recombination channel, the largest barrier being about 1.2 eV. To

2.4 Re/HZSM-5: a new catalyst for low temperature AmmoReform

While the conventional Degussa BMA process requires a high reaction temperature of ≥1200 °C, more recent studies show that the AmmoReform of light alkanes (ethane and propane from natural gas liquid) can be achieved at 600-700 °C.⁵⁸ This result demonstrated the possibility of achieving AmmoReform at relatively low temperatures (the same reaction temperature as the SteamReform and dry reforming). The efficient low-

temperature AmmoReform of ethane and propane was realized over the Re modified HZSM-5 zeolite rather than the conventional Pt-based catalyst for the BMA process. Fig. 5(a) shows the catalytic data of ethane AmmoReform over the Re/HZSM-5 performed at 650°C with a partial pressure ratio of $C_2H_6:NH_3:Ar = 0.25:0.5:0.25$ atm at a total flow of 40 ml/min. The mass-specific activities of H_2 , HCN, and N_2 (the primary products during ethane AmmoReform) increase almost linearly with increasing Re concentration (in HZSM-5) from 0 to 186 μ mol_Re/gcat. From the slopes of the linear equations, the

turnover frequency (TOF) of H_2 formation is up to 3.5 s⁻¹, and the TOF of AmmoReform, namely, the activity for HCN formation, is 0.8 s⁻¹. Additionally, the intercepts of such linear relations are approximately zero, suggesting that Re is the catalytically active site for AmmoReform, and the Brønsted acid sites of the HZSM-5 were not directly involved in the reaction. Without Re, pure HZSM-5 shows <1.5% ammonia conversion (through decomposition) and negligible ethane conversion under the same reaction conditions.⁵⁸

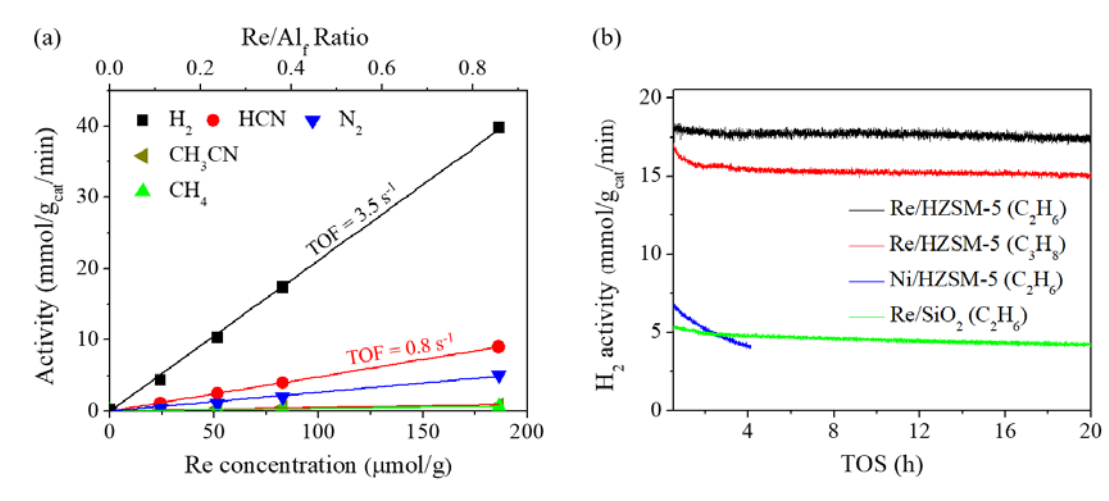


Figure 1 Catalytic data of ethane AmmoReform over the Re/HZSM-5 catalysts. Reproduced from ref. 58 with permission from American Chemical Society, Copyright © 2022 American Chemical Society.

The Re/HZSM-5 catalyst not only shows higher activity but also exhibits outstanding stability/coke-resistibility. Noteworthily, coke-induced catalyst deactivation is ubiquitous during the hydrocarbon transformation, especially over the acidic metal/zeolite catalysts. The Re/HZSM-5 is also an active catalyst for light alkane dehydrogenation and aromatization,71, ⁷² during which coke deposition is prevailing. Nonetheless, the Re/HZSM-5 catalyst is highly coke-resistant during the AmmoReform of both ethane and propane. As shown in Fig. 5(b), the activity of H₂ formation from ethane and propane AmmoReform over the Re/HZSM-5 (Re/Al_f = 0.2) remains stable within the time-on-stream (TOS) up to 20 h. According to the temperature-programmed oxidation (TPO) of the used catalysts,⁵⁸ coke deposition on the Re/HZSM-5 catalyst (after 20 h of TOS for ethane or propane AmmoReform) is negligible, indicating higher coke resistibility under the AmmoReform conditions, which must be associated with the presence of NH₃ as the co-reactant for light alkane conversion. It was hypothesized that the strong interaction between $NH_{\rm 3}$ and Brønsted/Lewis acid sites could prevent the oligomerization of olefins,⁵⁸ prohibiting the formation of polyaromatic species.⁷³

2.5 Re/HZSM-5 for AmmoReform: catalytic active structure and mechanism

The strictly linear relationship between activity and Re concentration strongly suggests that only one type of active site was formed for the Re/HZSM-5 catalysts with different Re loadings. In order to understand the structure of Re species in

HZSM-5 zeolite, the catalyst has been extensively characterized by X-ray absorption spectroscopy at Re L_{III}-edge, in-situ Raman spectroscopy, and HAADF-STEM.58 The formation of ReO₄tetrahedral (see Fig. 6 (d)), anchored to the framework AlfO₄⁻ (Al- O_f -Si) by replacing the Brønsted acid site in the 10MR (10membered ring) of the ZSM-5 zeolite, was expected for the fresh catalyst. 71, 72, 74-76 While the ReO_x oxo site can be easily reduced to Re⁰ clusters by hydrogen at 400 °C;⁷⁴ during the AmmoReform, such isolated oxo structure is only partially reduced despite the high H₂ partial pressure (up to 40% depending on the reaction conditions) under the AmmoReform reaction. The structure was hypothesized to be ReO_x (x≈2) (see Fig. 6 (e)), which was formed from the ReO₄- tetrahedral precursor during the early stage of the AmmoReform reaction. The formation of ReO_x ($x\approx2$) as the catalytically active structure was identified based on the quantitative analysis of the transient kinetic experiment during the early stage (see Fig. 6(a)), where a sharp peak of CO₂ and a broader peak of H₂O were observed. Quantification of the total desorbed O atom (in CO₂ and H₂O) suggested that nearly 50% of O in the ReO₄tetrahedral was removed. Noteworthily, the formation of HCN was delayed for about 18 seconds after introducing the reactants, and it takes up to 2.75 min to reach the steady state, demonstrating the significant influence of catalyst reconstruction on the ethane AmmoReform. A linear relationship between the mass-specific activity of HCN and the degree of oxygen defects was observed, indicating the pivotal role of the ReO_x ($x\approx2$) sites for AmmoReform.

The catalytic mechanism of ethane AmmoReform over the ReO_x oxo in HZSM-5 zeolite must be different from the aforementioned methane AmmoReform over the Pt-based catalysts under the BMA conditions. In order to elucidate the mechanism, the surface coverage of different species during the steady-state ethane AmmoReform has been quantified based on the time-dependent decay during the back-transient (the reactor influent was switched from reactants to inert).⁵⁸ Ammonia and HCN were found to dominate the surface/active sites of the catalyst during the reaction. The total specific amounts of NH_3 and HCN adsorbed on the Re/HZSM-5 catalyst

are 207 and 309 μ mol/g_{Cat}, respectively, corresponding to approximately 50% of coverage of Brønsted acid sites by NH₃ and 400% of coverage of Re-oxo by HCN, respectively. Based on this information, it is expected that the ReO_x (x≈2) site is octahedral coordinated with HCN or related intermediates (see Fig. 6(f)) during the reaction.⁵⁸ Further correlation of the early-stage activity with the surface carbon coverage and ethane partial pressure (see Fig. 6(c)) suggested that the reaction might follow the Eley-Rideal (C₂H₆ insertion) mechanism (Fig. 6(g)) because the activity increases linearly with increasing P_{ethane} rather than the surface carbon coverage.

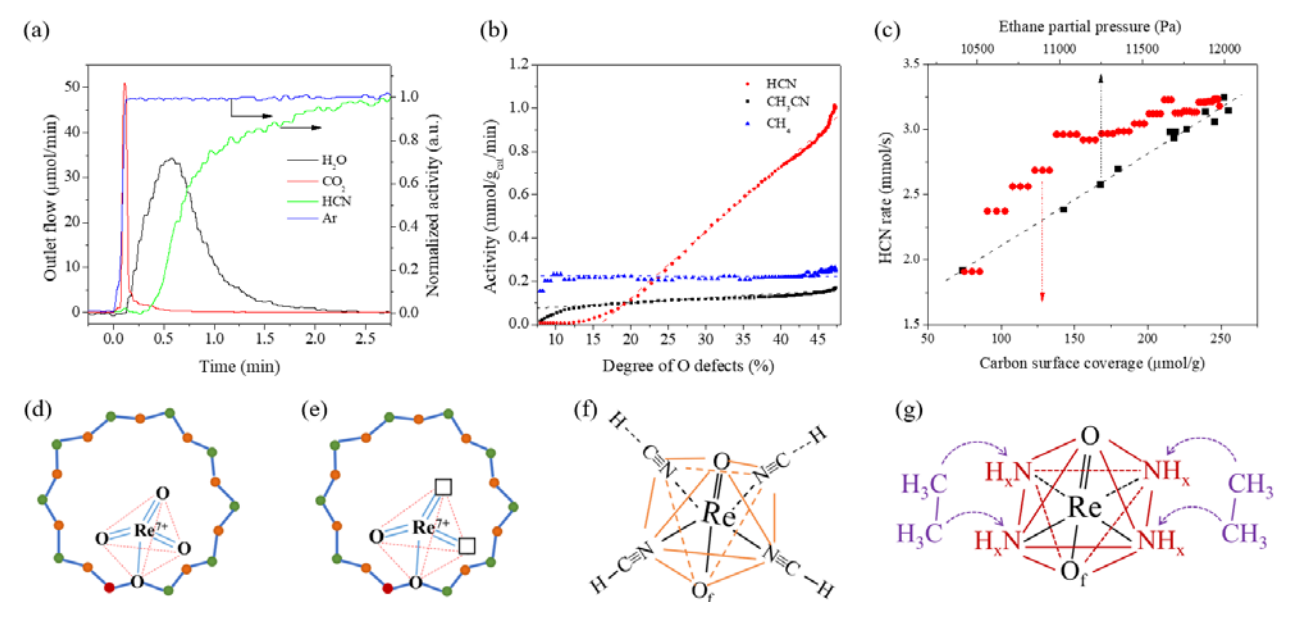


Figure 6 Transient kinetic results (a-c) and the structures of the Re species during ethane AmmoReform (d-g). (a) outlet flow of CO₂ and H₂O, and normalized outlet flow of HCN and inert standard (Ar) during the early-stage; (b) early-stage activities of HCN, CH₃CN, and CH₄ as a function of the degree of O defects; (c) HCN rate as a function of ethane partial pressure and surface carbon coverage. (d) structure of ReO₄⁻ tetrahedral anchored to the framework Al_fO₄⁻ (Al-O_f⁻-Si) in the fresh catalyst, (e) partially reduced ReO_x (x=2) structure after reaction, (f) possible "CN" coordinated ReO_x (x=2) structure during the steady-state AmmoReform, (g) hypothesized ethane insertion mechanism. Panels (a) and (b) were reproduced from ref. 58 with permission from American Chemical Society, Copyright © 2022 American Chemical Society.

3. Ammonia dehydrogenation for acetonitrile

3.1 Ammonia dehydrogenation and conventional ammoxidation

The catalytic reactions between ammonia and light alkane, in the absence of O_2 , can be achieved through not only the aforementioned AmmoReform but also ammonia dehydrogenation (AmmoDH) for ACN and H_2 . The concept of AmmoDH has been demonstrated in our recent publication and the reaction is realized through the tandem catalysis of dehydrogenative C-N coupling (dehydrogenation followed by amination).⁷³ Noteworthily, the AmmoDH discussed here is only for C_{2+} light alkane. The AmmoDH of methane actually is identical to the AmmoReform. The stoichiometric reaction of ethane AmmoDH is shown in equation (8).

$$C_2H_6 + NH_3 \rightarrow CH_3CN + 3H_2 \qquad \Delta H^{\circ} = 218.7 \text{ kJ}$$
 (8)

The oxidative ethane AmmoDH is well known as conventional ammoxidation (equation (9)).⁷⁷⁻⁸⁰

$$C_2H_6 + NH_3 + 1.5O_2 \rightarrow CH_3CN + 3H_2O(g)$$

 $\Delta H^{\circ} = -506.8 \text{ kJ}$ (9)

The same as AmmoReform, the AmmoDH is also highly endothermic and thermodynamically favored at higher reaction temperatures (see Fig. 7). The reactions (1), (3), (4), (5), and (7) mentioned in section 2.1 for AmmoReform are involved as the side reactions during the AmmoDH. As aforementioned, these side reactions (equations (3)-(5) and (7)) have negative ΔG at temperatures between 300-800 $^{\circ}C$.

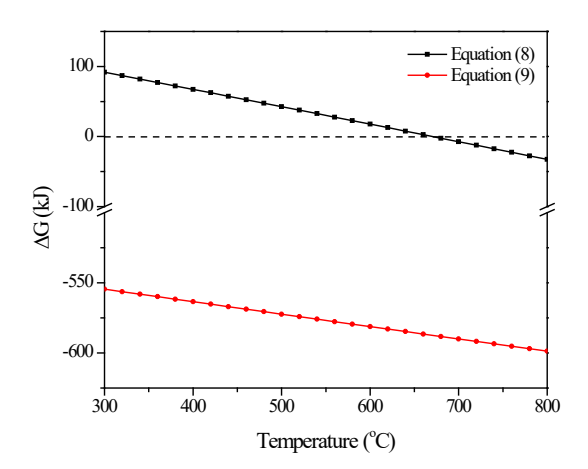


Figure 7 Gibbs free energy change as a function of reaction temperature for ethane AmmoDH (equation (8) and ammoxidation (equation (9)). Calculated using HSC Chemistry 6.0.

In contrast, the conventional ammoxidation is highly exothermic with free energy $\Delta G < -550$ kJ. In principle, a high conversion can be achieved at relatively mild temperatures. Additionally, coke deposition during the oxidative process is usually less significant than the nonoxidative process. For example, ACN and ethylene were produced from ethane ammoxidation over the mixed metal oxide81-85 or Co-exchanged zeolite77-79, 86-90 catalysts. Although conventional ammoxidation produces the same type of product as the AmmoDH from the light alkane, these two reactions are fundamentally different. It was mentioned by Li and Armor,86 in their pioneer work on the Co/zeolite for ethane ammoxidation, "In the absence of O_2 , no reaction occurs". Therefore, the ammoxidation involves different catalytic mechanisms from the AmmoDH for light alkane conversion. We also noticed that the AmmoDH catalyst is incompetent for ammoxidation, in the presence of O_2 , a significant amount of CO₂ was produced. Additionally, up to 70% of the converted NH₃ was oxidized to NO_x during ammoxidation,88 of which is absent from the AmmoDH.

3.2. Bifunctional catalyst enables AmmoDH

While it is promising to produce ACN and H_2 directly from ammonia and ethane, such a reaction was less concerning than the ammoxidation, most likely due to the lack of an active catalyst under the anaerobic conditions. Specifically, the AmmoDH reaction must be achieved at relatively low temperatures, because the reaction is dominated by C-C cleavage and turned to AmmoReform at high temperatures. Therefore, an efficient catalyst for low-temperature dehydrogenation is essential. To the best of our knowledge, the only attempt at the anaerobic reaction between light alkanes and ammonia at lower temperatures was made by Denton and Bishop 70 years ago, which was not quite successful over their investigated MoO_3/Al_2O_3 catalyst due to the low activity.

Recent efforts by our group in ethane AmmoDH show that the metal/acid bifunctional catalysts are highly efficient.⁷³ The reaction is realized through metal sites catalyzed ethane dehydrogenation followed by ethylene amination (with NH₃) on the acid sites, namely a tandem dehydrogenative C-N coupling

mechanism (see Fig. 8(a)). It is well known that transition metals, such as Pt, are highly active in ethane dehydrogenation to ethylene. Additionally, the amination reaction of ethylene with ammonia can be realized on the Brønsted acid sites of the zeolite through the ammonia insertion mechanism.^{73, 92, 93} Finally, the dehydrogenation of ethylamine leads to the formation of ACN. The direct formation of ACN from ethylene and ammonia through amination followed by dehydrogenation has also been investigated.94 Low temperatures are preferred for such a tandem catalytic process since the formation of CH₄ and HCN is favored at high reaction temperatures (the reaction turned to AmmoReform).73 Additionally, the C-N coupling between NH₃ and C₂H₄ through amination is also favored at low temperatures (preferably at high pressure). Consequently, a metal site (with high dehydrogenation activity at relatively low temperatures) in combination with a strong Brønsted acid site is essential for the AmmoDH catalyst.

Based on the hypothesized mechanistic pathway, the Pt/HZSM-5 has been identified as the active catalyst for ethane AmmoDH at temperatures as low as 350°C. The specific rate of ACN at such a low temperature is ~60 μmol/g/min (or 12 mmol/g_{Pt}/min), and as shown in Fig. 8 (b-c), the selectivity of ACN is up to 99%, although at very low ethane and ammonia conversion (~1%). The low conversion is due to both kinetic and thermodynamic limitations. The conversion increases with increasing temperature, however, the selectivity decreases. In comparison to other catalytic systems for ethane conversions, such as dehydroaromatization, dehydrogenation, and ammoxidation, the Pt/HZSM-5 catalyzed AmmoDH is more efficient.73 The activity of ethane AmmoDH is significantly higher than the ammoxidation over the Co/β catalyst (compared at 500°C).^{77, 86} Indeed, the Pt/HZSM-5 (employed for ethane AmmoDH) is also a conventional catalyst for ethane dehydrogenation or dehydroaromatization (if ammonia is removed from the reactant mixture). Direct comparison between AmmoDH with dehydrogenation over the same 0.5 wt% Pt/HZSM-5 catalyst under identical conditions at 400°C show that the reaction rate of ethane during the AmmoDH is more than twice that for the dehydrogenation.73 Therefore, it might be concluded that the presence of ammonia assists ethane dehydrogenation.

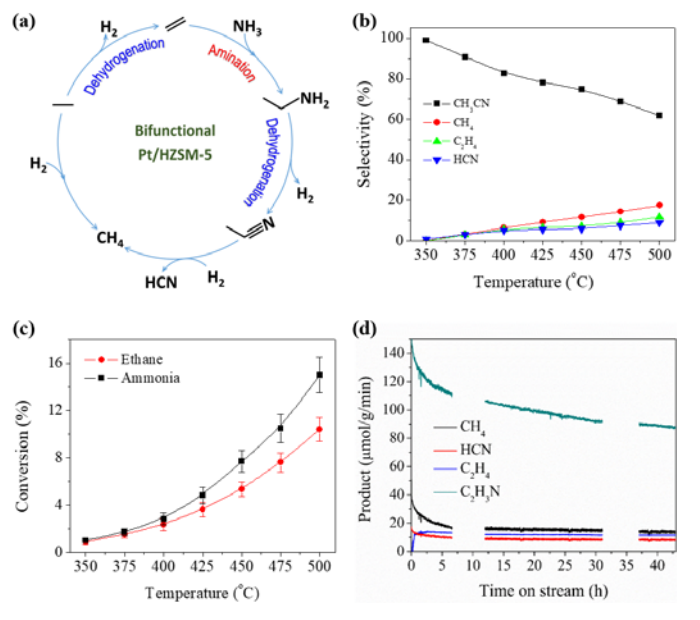


Figure 8. (a) Schematic illustration of the tandem dehydrogenative C-N coupling mechanism; (b)-(d) catalytic results of ethane AmmoDH over 0.5 wt% Pt/HZSM-5 catalyst. (b)-(c): influence of reaction temperature on selectivity and conversion, (d): time on stream behavior (stability) of the catalyst. Reproduced from ref. 73 with permission from American Chemical Society, Copyright © 2021 American Chemical Society.

Another intriguing observation of AmmoDH is that the presence of ammonia as a reactant during the AmmoDH, in principle, could decrease the rate of coking. As aforementioned in the AmmoReform section, it remains a key challenge to avoid the ubiquitous coke deposition during light alkanes conversion under anaerobic conditions. Interestingly, due to the strong interactions between ammonia and the Lewis/Brønsted acid sites of the Pt/HZSM-5 catalyst, the formation of heavier reaction intermediates (coke precursors) from the oligomerization of ethylene intermediate on the acid sites of the catalyst is prohibited. Therefore, the AmmoDH shows higher stability/coke-resistibility than the other anaerobic reaction

processes, especially the dehydroaromatization.⁷³ The stability of the Pt/HZSM-5 catalyst in the ethane AmmoDH has been studied at 400° C (see Fig. 8(d)). The rate of ACN only decreased from ~140 to 90 μ mol/g_{cat}/min after time on stream up to 42 h.

3.3. Metal/acid bifunctionality needs to be optimized

While the benchmark Pt/HZSM-5 shows promising activity and stability in ethane AmmoDH, the proposed bifunctional tandem dehydrogenative C-N coupling mechanism (see Fig. 8(a)) strongly suggested that the catalytic performance can be further optimized by tuning the metal and acid functionalities of the catalyst. It is expected that the key to the activity/selectivity of AmmoDH is the interactions between NH₃ and the catalyst: such interaction should be "just right" as suggested by the Sabatier principle.95 For example, if the interaction between NH₃ and catalytic active sites is too strong, then the initial C-H bond activation must be prohibited. Therefore, it is essential to tune the chemical properties of the metal sites in the zeolite. Various second metals, including Co, Zn, Ga, In, Sn, Ce, Rh, Zr, Mn, and Pd, have been employed to tune the metal/acid functionalities of the catalyst for ethane AmmoDH, the Co modified Pt/HZSM-5 catalyst has been identified with enhanced activity, selectivity, and stability, simultaneously.94 Noteworthily, the Co/HZSM-5 is also an active catalyst for ethane ammoxidation,78,79 however, is inactive (produces negligible acetonitrile and ethylene at 600°C) for ethane AmmoDH under anaerobic conditions.94 Therefore, Co is considered a promoter, modifying the metal and acid functionalities of the Pt/HZSM-5 catalyst. In order to understand the promotion effect of Co on the Pt/HZSM-5 catalyst for ethane AmmoDH, future research is necessary to address scientific questions, such as what are the relationships between the chemical properties (structure, composition, and siting) of Pt and Co species and the catalytic reactivity; and how does the Brønsted acid density of the zeolite host influence the structure and catalytic performance of the Pt and Co sites.

ARTICLE

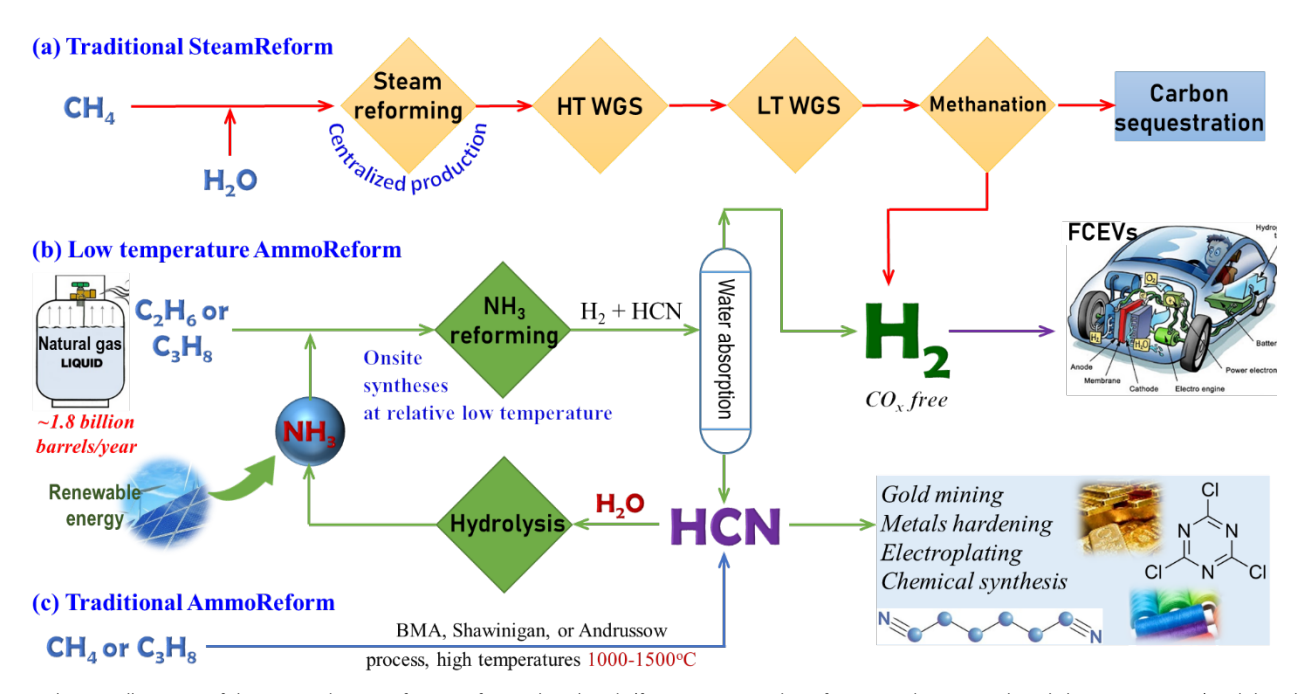


Figure 9 Schematic illustration of the proposed ammoreforming of natural gas liquids (for onsite HCN and CO_x-free H₂ production at relatively low temperatures) and the related conventional processes.

4. New opportunities and challenges for AmmoReform and AmmoDH

4.1 AmmoReform for CO_x-free H₂

The efficient AmmoReform of ethane and propane, catalyzed by Re/HZSM-5, at the temperature range for the conventional SteamReform provides new opportunities for this old catalytic reaction. A schematic illustration of the industrial significance of the low-temperature AmmoReform of ethane and propane and its related conventional processes is shown in Fig. 9. Specifically, the AmmoReform at the same temperatures as the $conventional\,Steam Reform\,makes\,it\,feasible\,for\,the\,on\text{-}purpose$ H₂ production (with HCN as the by-product). The absence of CO_x is a significant advantage in contrast to the SteamReform for H₂ production. As demonstrated in Fig. 9 (path (a)), methane SteamReform produces stoichiometric amounts of CO or CO₂, which imposes additional costs for CO₂ sequestration and CO transformation: through two stages of the water-gas-shift reaction, an additional methanation reactor is required to produce CO_x free H_2 for the PEMFCs. Whereas, the AmmoReform produces HCN (instead of CO and CO₂) as the coproduct, which can be easily removed through water adsorption as developed for the Andrussow process. The costs of H2 purification during the AmmoReform must be significantly

lower than the conventional SteamReform. According to techno-economic analysis (TEA), the pressure swing adsorption (for H_2 purification), during the conventional SteamReform using a packed-bed reactor, is the most critical economic parameter.⁹⁶

The key limitation of AmmoReform is that ammonia is currently still mainly produced with hydrogen from methane SteamReform. The opportunity of AmmoReform for CO_x -free H_2 production relies on green ammonia production from renewable energy. Indeed, ammonia as a carbon-free H_2 carrier has been extensively recognized recently. $^{51-53}$ A systematic TEA of hydrogen transportation infrastructure using ammonia and methanol reveals that the cost of transporting hydrogen using ammonia (\$1479/t-H₂) is cheaper than using methanol (\$1879/t-H₂). 97 As demonstrated in Fig. 7 (path (b)), AmmoReform could be an alternative process for on-site CO_x -free H_2 production because both ammonia and C_{2+} light alkane can be transported in liquid form (NH₃ and C_{2+} alkane can be liquefied at pressure < 40 atm) when green ammonia becomes ubiquitously available from renewable energy.

In contrast to ammonia decomposition, the proposed AmmoReform aims at the efficient conversion of cheap and abundant light alkane. Although significant increase in renewable energy utilization, fossil energy (with appropriate CO₂ capture) will still play a critical role in the chemical and

energy sectors in the near future. Therefore, the AmmoReform (utilizing both fossil light alkane and renewable ammonia) might play a role during the transition period. Direct comparison between light alkane AmmoReform and ammonia decomposition is not the focal area of this perspective.

Another challenge is that the market size of H_2 is significantly large compared with the by-product HCN. The proposed AmmoReform alone certainly will not meet the demand for the future H_2 economy. However, it might be a complement to the conventional SteamReform and other techniques, especially for on-site CO_x -free H_2 production. Additionally, new catalytic processes for HCN transformation, such as catalytic hydrolysis (HCN + $H_2O \rightarrow NH_3 + CO^{98-100}$ or $NaCN + H_2O \rightarrow HCOONa + NH_3^{101, 102}$) must be developed to convert HCN back to NH_3 and/or other chemicals and intermediates. Although HCN hydrolysis has been studied previously, such a process is not being used in industry and the process is of interest only for exhaust gas treatment currently.

While the low-temperature AmmoReform provides a new opportunity for on-purpose CO_x -free H_2 production, a systematic TEA and life cycle assessment (LCA) of such a process is waiting to be evaluated. Regardless of its potential for H_2 production, the application of low-temperature AmmoReform must benefit when considering HCN as the target product (for on-site synthesis). In terms of the catalyst, the present Re/HZSM-5 is active only for C_{2+} light alkane (ethane and propane) AmmoReform, most likely due to the fundamental difference from the Pt-catalyzed Degussa BMA process in terms of mechanism. New catalysts for methane AmmoReform are waiting to be developed and catalyst stability under industrially relevant conditions is also waiting to be studied.

4.2 AmmoDH for on-purpose acetonitrile production

The direct reaction between ethane and ammonia under milder conditions through AmmoDH provides an alternative method for on-purpose ACN production. Acetonitrile is a saturated aliphatic nitrile with a low freezing point, low toxicity, and low viscosity. It has medium polarity and exhibits excellent solubility to both polar and non-polar compounds. Therefore, it has been widely used as a solvent in the battery (because of its relatively high dielectric constant), refineries (an extractor for butadiene purification), and other organic synthesis. Besides its main application as a solvent, ACN is also a common building block in organic synthesis. Acetonitrile can be converted through hydrogenation into ethylamine, 103 which has an annual global market of 1.85×10^5 tons. 104 lt can also be converted through hydrolysis into acetic acid and acetamide. 105 Therefore, it can be used as the precursor to medicines, pesticides, and paints. While in the current industry, acetonitrile is recovered (as a byproduct) during the propylene ammoxidation (SOHIO Process) that aims at acrylonitrile production, the on-purpose AmmoDH for acetonitrile production from the abundant ethane or ethylene could be an important alternative. Additionally, the AmmoDH co-produces significant amounts of H2 (about three times of total useful carbon-based products), which can be used for the subsequent ACN hydroconversion.

The same as the concept of AmmoReform for CO_x -free H_2 production, the AmmoDH is also a new concept that requires systematical TEA and LCA evaluations. The key limitation might be the small market size of ACN, which calls for the development of new catalytic processes for ACN upgrading through hydrogenation and hydrolysis. Additionally, a more efficient catalyst is also waiting to be developed, which relies on the fundamental understanding of the metal/acid bifunctionality during such a tandem catalytic process.

5. Conclusion

The unprecedented increase in shale gas production provided cheaper and more abundant light alkane as the feedstock for chemicals and fuel syntheses. In industry, light alkane was mainly co-processed with steam (H2O (g)) through cracking (for ethylene) or reforming (for H₂). Alternative to the steamassisted conversion process, green ammonia from renewable energy, which has been considered an important energy carrier, could be an alternative co-reactant for efficient light alkane conversion. This perspective intends to accentuate the essentials of two ammonia-assisted light alkane conversion processes, namely AmmoReform (for CO_x-free H₂ and HCN) and AmmoDH (or dehydrogenative C-N coupling for ACN and H₂). Specifically, a comprehensive exploration of the early industrial process related to the Degussa BMA process (for HCN production), which is the only industry process related to the ammonia-assisted light alkane conversion, was carried out. Then the current state-of-the-art knowledge of the catalytic systems of both AmmoReform and AmmoDH was addressed. With the assistance of the Re/HZSM-5 catalyst, the AmmoReform, which was carried out at temperatures up to 1200°C during the BMA process, can be realized at the same temperature range as SteamReform. Therefore, the new opportunity and challenge of AmmoReform toward CO_x-free H₂ production was discussed. Moreover, through optimizing the metal/acid bifunctionality, ethane direct dehydrogenative C-N coupling with ammonia (the AmmoDH process) can be realized at temperatures as low as 350°C. Such a reaction produces ACN directly from ethane and ammonia under anaerobic conditions and shows a significantly higher rate than the conventional ammoxidation process; therefore, it might be an important alternative for on-purpose ACN production. As green ammonia from renewable energy becomes ubiquitously available, coprocessing light alkane with ammonia through the discussed AmmoReform and AmmoDH might emerge as new platform reactions for chemicals and energy transformations.

Conflicts of interest

There are no conflicts to declare.

Acknowledgements

Y.X. is grateful for the financial support from the National Science Foundation (#2210760 and #2247058) for the projects of ammonia-assisted light alkane conversion.

Notes and references

- 1 https://www.eia.gov/tools/faqs/faq.php?id=52&t=8.
- 2 https://www.eia.gov/energyexplained/natural-gas/how-much-gas-is-left.php.
- S. Ahn, P. Littlewood, Y. Liu, T. J. Marks and P. C. Stair, ACS Catal, 2022, 12, 10522-10530.
- 4 C. Palmer, D. C. Upham, S. Smart, M. J. Gordon, H. Metiu and E. W. McFarland, *Nat Catal*, 2020, **3**, 83-89.
- 5 Y. Song, Y. He and S. Laursen, ACS Catalysis, 2020, 10, 8968-8980.
- 6 Y. Song, E. Ozdemir, S. Ramesh, A. Adishev, S. Subramanian, A. Harale, M. Albuali, B. A. Fadhel, A. Jamal, D. Moon, S. H. Choi and C. T. Yavuz, *Science*, 2020, **367**, 777-781.
- S. Penner and P. D. Kheyrollahi Nezhad, ACS Catal, 2021, 11, 5271-5286.
- 8 A. I. Tsiotsias, N. D. Charisiou, V. Sebastian, S. Gaber, S. J. Hinder, M. A. Baker, K. Polychronopoulou and M. A. Goula, *Int J Hydrog Energy*, 2022, 47, 5337-5353.
- 9 R. Ryoo, J. Kim, C. Jo, S. W. Han, J.-C. Kim, H. Park, J. Han, H. S. Shin and J. W. Shin, *Nature*, 2020, 585, 221-224.
- 10 R. T. Hannagan, G. Giannakakis, R. Réocreux, J. Schumann, J. Finzel, Y. Wang, A. Michaelides, P. Deshlahra, P. Christopher, M. Flytzani-Stephanopoulos, M. Stamatakis and E. C. H. Sykes, *Science*, 2021, 372, 1444-1447.
- 11 A. H. Motagamwala, R. Almallahi, J. Wortman, V. O. Igenegbai and S. Linic, *Science*, 2021, **373**, 217-222.
- 12 L. Qi, M. Babucci, Y. Zhang, A. Lund, L. Liu, J. Li, Y. Chen, A. S. Hoffman, S. R. Bare, Y. Han, B. C. Gates and A. T. Bell, *J Am Chem Soc*, 2021, **143**, 21364-21378.
- 13 H. Yan, K. He, I. A. Samek, D. Jing, M. G. Nanda, P. C. Stair and J. M. Notestein, *Science*, 2021, **371**, 1257-1260.
- 14 D. Zhao, X. Tian, D. E. Doronkin, S. Han, V. A. Kondratenko, J. D. Grunwaldt, A. Perechodjuk, T. H. Vuong, J. Rabeah, R. Eckelt, U. Rodemerck, D. Linke, G. Jiang, H. Jiao and E. V. Kondratenko, *Nature*, 2021, 599, 234-238.
- 15 H. Zhou, X. Yi, Y. Hui, L. Wang, W. Chen, Y. Qin, M. Wang, J. Ma, X. Chu, Y. Wang, X. Hong, Z. Chen, X. Meng, H. Wang, Q. Zhu, L. Song, A. Zheng and F.-S. Xiao, *Science*, 2021, **372**, 76-80
- X. Jiang, B. M. Lis, S. C. Purdy, S. Paladugu, V. Fung, W. Quan,
 Z. Bao, W. Yang, Y. He, B. G. Sumpter, K. Page, I. E. Wachs and
 Z. Wu, ACS Catalysis, 2022, 12, 11239-11252.
- L. Ni, R. Khare, R. Bermejo-Deval, R. Zhao, L. Tao, Y. Liu and J. A. Lercher, *J Am Chem Soc*, 2022, **144**, 12347-12356.
- 18 J. Shan, M. Li, L. F. Allard, S. Lee and M. Flytzani-Stephanopoulos, *Nature*, 2017, **551**, 605-608.
- 19 V. L. Sushkevich, D. Palagin, M. Ranocchiari and J. A. van Bokhoven, *Science*, 2017, **356**, 523-527.
- 20 R. Jin, M. Peng, A. Li, Y. Deng, Z. Jia, F. Huang, Y. Ling, F. Yang, H. Fu, J. Xie, X. Han, D. Xiao, Z. Jiang, H. Liu and D. Ma, *J Am Chem Soc*, 2019, **141**, 18921-18925.
- 21 Z. Jin, L. Wang, E. Zuidema, K. Mondal, M. Zhang, J. Zhang, C. Wang, X. Meng, H. Yang, C. Mesters and F.-S. Xiao, *Science*, 2020, **367**, 193-197.
- 22 A. Koishybay and D. F. Shantz, J Am Chem Soc, 2020, 142, 11962-11966.
- 23 Z. Liu, E. Huang, I. Orozco, W. Liao, R. M. Palomino, N. Rui, T. Duchoň, S. Nemšák, D. C. Grinter, M. Mahapatra, P. Liu, J. A. Rodriguez and S. D. Senanayake, *Science*, 2020, **368**, 513-517.
- 24 M. C. Simons, S. D. Prinslow, M. Babucci, A. S. Hoffman, J. Hong, J. G. Vitillo, S. R. Bare, B. C. Gates, C. C. Lu, L. Gagliardi and A. Bhan, *J Am Chem Soc*, 2021, **143**, 12165-12174.

- 25 A. J. Heyer, D. Plessers, A. Braun, H. M. Rhoda, M. L. Bols, B. Hedman, K. O. Hodgson, R. A. Schoonheydt, B. F. Sels and E. I. Solomon, *J Am Chem Soc*, 2022, **144**, 19305-19316.
- 26 E. Gomez, X. Nie, J. H. Lee, Z. Xie and J. G. Chen, J Am Chem Soc, 2019, 141, 17771-17782.
- 27 F. Goodarzi, D. B. Christensen, F. Joensen, S. Kegnæs and J. Mielby, Appl Catal A, 2020, 592, 117383.
- 28 A. Caiola, B. Robinson, X. Bai, D. Shekhawat and J. Hu, *Ind Eng Chem Res*, 2021, **60**, 11421-11431.
- 29 C.-W. Chang, H. N. Pham, R. Alcala, A. K. Datye and J. T. Miller, ACS Sustain Chem Eng, 2021, 10, 394-409.
- 30 Y. Liu, M. Ćoza, V. Drozhzhin, Y. van den Bosch, L. Meng, R. van de Poll, E. J. M. Hensen and N. Kosinov, *ACS Catal*, 2022, **13**, 1-10
- 31 T. Sumi, S. Kokuryo, Y. Fujimoto, X. Li, K. Miyake, Y. Uchida and N. Nishiyama, *Catal Sci Technol*, 2022, **12**, 7010-7017.
- 32 T. Liang, H. Toghiani and Y. Xiang, *Ind Eng Chem Res*, 2018, 57, 15301-15309.
- 33 Y. Xiang, H. Wang, J. Cheng and J. Matsubu, *Catal Sci Technol*, 2018, **8**, 1500-1516.
- 34 T. Liang, S. Fadaeerayeni, J. Shan, T. Li, H. Wang, J. Cheng, H. Toghiani and Y. Xiang, *Ind Eng Chem Res*, 2019, **58**, 17699-17708.
- 35 S. Fadaeerayeni, G. Chen, H. Toghiani and Y. Xiang, *Top Catal*, 2020. **63**. 1463-1473.
- 36 S. Fadaeerayeni, J. Shan, E. Sarnello, H. Xu, H. Wang, J. Cheng, T. Li, H. Toghiani and Y. Xiang, Appl Catal A, 2020, 601, 117629.
- 37 G. Chen, L. Fang, T. Li and Y. Xiang, *J Am Chem Soc*, 2022, **144**, 11831-11839.
- 38 J. D. Idol, US 2,904,580, 1959.
- 39 B. Cornils, in *Catalysis from A to Z* (eds W. Herrmann, B. Cornils, H. Zanthoff and J.-H. Xu), 2020, DOI: https://doi.org/10.1002/9783527809080.cataz04849.
- 40 J. Sauer, M. Bewersdorf, M. Köstner, M. Rinner and D. Wolf, in *Handbook of Heterogeneous Catalysis*, 2008, DOI: https://doi.org/10.1002/9783527610044.hetcat0131, pp. 2592-2609.
- 41 F. Endter, Chem Ing Tech, 1958, 30, 305-310.
- 42 E. Koberstein, Ind Eng Chem Process Des Dev, 1973, 12, 444-448.
- 43 S. Delagrange and Y. Schuurman, *Catal Today*, 2007, **121**, 204-209.
- 44 S. S. Bharadwaj and L. D. Schmidt, *Ind Eng Chem Res*, 1996, **35**, 1524-1533.
- 45 B. Y. K. Pan and R. G. Roth, Ind Eng Chem Process Des Dev, 1968, **7**, 53-61.
- 46 G. J. Hutchings, Appl Catal, 1986, 28, 7-11.
- 47 A. G. Dietz Iii and L. D. Schmidt, Appl Catal A, 1999, 180, 287-298.
- 48 Chemical & Engineering News, 1961, **39**, 1. doi: 10.1021/cenv039n041.p001
- 49 in Ullmann's Encyclopedia of Industrial Chemistry, Gail, E., Gos, S., Kulzer, R., Lorösch, J., Rubo, A., Sauer, M., Kellens, R., Reddy, J., Steier, N. and Hasenpusch, W. (2011). Cyano Compounds, Inorganic. In Ullmann's Encyclopedia of Industrial Chemistry, (Ed.). doi:10.1002/14356007.a08_159.pub3.
- 50 D. Ye and S. C. E. Tsang, Nat Syn, 2023, 2, 612-623.
- 51 F. Schüth, R. Palkovits, R. Schlögl and D. S. Su, *Energy & Environ Sci*, 2012, **5**, 6278-6289.
- 52 R. F. Service, Ammonia—a renewable fuel made from sun, air, and water—could power the globe without carbon, DOI: doi: 10.1126/science.aau7489).
- 53 D. R. MacFarlane, P. V. Cherepanov, J. Choi, B. H. R. Suryanto, R. Y. Hodgetts, J. M. Bakker, F. M. Ferrero Vallana and A. N. Simonov, *Joule*, 2020, **4**, 1186-1205.
- 54 https://www.cnn.com/2022/10/18/africa/green-ammonia-hive-energy-scn-climate-spc-intl/index.html.

- 55 https://e360.yale.edu/features/from-fertilizer-to-fuel-can-green-ammonia-be-a-climate-fix.
- 56 https://www.ammoniaenergy.org/articles/engie-siemens-ecuity-and-stfc-publish-feasibility-of-ammonia-to-hydrogen/.
- 57 https://www.chevron.com/newsroom/2022/q4/air-liquide-chevron-lyondellbasell-and-uniper-to-pursue-lower-carbon-hydrogen-and-ammonia-project.
- 58 S. Fadaeerayeni, X. Yu, E. Sarnello, Z. Bao, X. Jiang, R. R. Unocic, L. Fang, Z. Wu, T. Li and Y. Xiang, *ACS Catal*, 2022, **12**, 3165-3172.
- 59 C. Voigt, P. Kleinschmit, E. Walter, US 4,289,741, 1981.
- 60 C. Hecht, P. Panster, F. Bittner, P. Look-Herber, DE3923034A1, 1989.
- 61 S. Lee, Energy Technol, 2013, 1, 419-420.
- 62 W. A. Hillebrand, Ind Eng Chem Pro Res Dev, 1984, 23, 476-479.
- 63 L. C. Grabow, F. Studt, F. Abild-Pedersen, V. Petzold, J. Kleis, T. Bligaard and J. K. Nørskov, Angew Chem Int Ed, 2011, 50, 4601-4605.
- 64 D. Hasenberg and L. D. Schmidt, J Catal, 1985, 91, 116-131.
- 65 D. Hasenberg and L. D. Schmidt, J Catal, 1986, 97, 156-168.
- 66 E. Herceg and M. Trenary, *J Am Chem Soc*, 2003, **125**, 15758-15759.
- 67 E. Herceg and M. Trenary, J Phys Chem B, 2005, 109, 17560-17566.
- 68 M. Diefenbach, M. Brönstrup, M. Aschi, D. Schröder and H. Schwarz, *J Am Chem Soc*, 1999, **121**, 10614-10625.
- 69 M. Aschi, M. Brönstrup, M. Diefenbach, J. N. Harvey, D. Schröder and H. Schwarz, Angew Chem Int Ed, 1998, 37, 829-832
- 70 J. Gómez-Díaz and N. López, *J Phys Chem C*, 2011, **115**, 5667-5674.
- 71 H. S. Lacheen, P. J. Cordeiro and E. Iglesia, J Am Chem Soc, 2006, 128, 15082-15083.
- 72 Y. Wu, S. Holdren, Y. Zhang, S. C. Oh, D. T. Tran, L. Emdadi, Z. Lu, M. Wang, T. J. Woehl, M. Zachariah, Y. Lei and D. Liu, J Catal, 2019, 372, 128-141.
- 73 G. Chen, T. Liang, P. Yoo, S. Fadaeerayeni, E. Sarnello, T. Li, P. Liao and Y. Xiang, *ACS Catal*, 2021, **11**, 7987-7995.
- 74 H. S. Lacheen, P. J. Cordeiro and E. Iglesia, *Chem Eur J*, 2007, **13**. 3048-3057.
- 75 S. Lwin, C. Keturakis, J. Handzlik, P. Sautet, Y. Li, A. I. Frenkel and I. E. Wachs, *ACS Catal*, 2015, 5, 1432-1444.
- 76 B. Zhang and I. E. Wachs, ACS Catal, 2021, 11, 1962-1976.
- 77 Y. Li and J. N. Armor, Chem Commun, 1997, 20, 2013-2014.
- 78 Y. Li and J. N. Armor, *J Catal*, 1998, **176**, 495-502.
- 79 X. Liu, T. Liang, R. Barbosa, G. Chen, H. Toghiani and Y. Xiang, *ACS Omega*, 2020, **5**, 1669-1678.
- 80 T. Liang, X. Liu, Y. He, R. Barbosa, G. Chen, W. Fan and Y. Xiang, Appl Catal A, 2021, **610**, 117942.
- S. M. Aliev and V. D. Sokolovskii, React Kinet Catal Lett, 1978, 9, 91-97.
- 82 E. V. Ischenko, T. V. Andrushkevich, G. Y. Popova, V. M. Bondareva, Y. A. Chesalov, T. Y. Kardash, L. M. Plyasova, L. S. Dovlitova and A. V. Ischenko, in *Studies in Surface Science and Catalysis*, eds. E. M. Gaigneaux, M. Devillers, S. Hermans, P. A. Jacobs, J. A. Martens and P. Ruiz, Elsevier, 2010, vol. 175, pp. 479-482.
- 83 T. T. Nguyen, L. Burel, D. L. Nguyen, C. Pham-Huu and J. M. M. Millet, *Appl Catal A*, 2012, **433-434**, 41-48.
- 84 E. Rojas, J. J. Delgado, M. O. Guerrero-Pérez and M. A. Bañares, *Catal Sci Technol*, 2013, **3**, 3173-3182.
- 85 M.-J. Cheng and W. A. Goddard, J Am Chem Soc, 2015, **137**, 13224-13227.
- 86 Y. Li and J. N. Armor, J Catal, 1998, 173, 511-518.
- 87 Y. Li and J. N. Armor, Appl Catal A, 1999, 183, 107-120.
- 88 Y. Li and J. N. Armor, Appl Catal A, 1999, 188, 211-217.

- 89 Z. Sobalík, A. A. Belhekar, Z. Tvarůžková and B. Wichterlová, Appl Catal A, 1999, **188**, 175-186.
- 90 B. Wichterlová, Z. Sobalík, Y. Li and J. N. Armor, in *Studies in Surface Science and Catalysis*, eds. A. Corma, F. V. Melo, S. Mendioroz and J. L. G. Fierro, Elsevier, 2000, vol. 130, pp. 869-874.
- 91 W. I. Denton and R. B. Bishop, *Ind Eng Chem*, 1953, **45**, 282-286.
- 92 M. Deeba, M. E. Ford and T. A. Johnson, *J Chem Soc, Chem Commun*, 1987, 562-563.
- 93 C. R. Ho, L. A. Bettinson, J. Choi, M. Head-Gordon and A. T. Bell, *ACS Catal*, 2019, **9**, 7012-7022.
- 94 G. Chen, S. Fadaeerayeni, L. Fang, E. Sarnello, T. Li, H. Toghiani and Y. Xiang, *Catal Today*, 2023, **416**.
- 95 P. Sabatier, Ber Dtsch Chem Ges, 1911, 44, 1984-2001.
- 96 H. Lee, B. Lee, M. Byun and H. Lim, *Chem Eng Res Design*, 2021, **171**, 383-394.
- 97 J. Cui and M. Aziz, Int J Hydrogen Energy, 2023, 48, 15737-
- 98 O. Kröcher and M. Elsener, Appl Catal B, 2009, 92, 75-89.
- 99 L. Yan, S. Tian, J. Zhou and X. Yuan, Front Environ Sci Eng, 2016, 10. 5.
- Z. Song, Q. Zhang, P. Ning, Y. Wang, Y. Duan, J. Wang and
 Huang, RSC Adv, 2016, 6, 111389-111397.
- 101 G. W. Heise and H. E. Foote, J Ind Eng Chem, 1920, 12, 331-336.
- 102 H. Sulzer, Angew. Chem., 1912, 25, 1268-1273.
- 103 N. Iwasa, M. Yoshikawa and M. Arai, *Phys Chem Chem Phys*, 2002, **4**, 5414-5420.
- 104 R. Xia, D. Tian, S. Kattel, B. Hasa, H. Shin, X. Ma, J. G. Chen and F. Jiao, *Nat Commun*, 2021, **12**, 1949.
- 105 L. A. M. M. Barbosa and R. A. van Santen, J Catal, 2000, 191, 200-217.